Available online at www.sciencedirect.com
ScienceDirect
Journal of Nuclear Materials 372 (2008) 379–390
journal of nuclear materials
www.elsevier.com/locate/jnucmat

# Effect of irradiation-induced plastic flow localization on ductile crack resistance behavior of a 9%Cr tempered martensitic steel

R. Chaouadi *,[1]

*Forschungszentrum Jülich, EURATOM Association, IEF-2, D-52425 Jülich, Germany*

Received 29 November 2006; accepted 19 April 2007

**Abstract**

This paper examines the effect of irradiation-induced plastic flow localization on the crack resistance behavior. Tensile and crack resistance measurements were performed on Eurofer-97 that was irradiated at 300 °C to neutron doses ranging between 0.3 and 2.1 dpa. A severe degradation of crack resistance behavior is experimentally established at quasi-static loading, in contradiction with the Charpy impact data and the dynamic crack resistance measurements. This degradation is attributed to the dislocation channel deformation phenomenon. At quasi-static loading rate, scanning electron microscopy observations of the fracture surfaces revealed a significant change of fracture topography, mainly from equiaxed dimples (mode I) to shear dimples (mode I + II). With increasing loading rate, the high peak stresses that develop inside the process zone activate much more dislocation sources resulting in a higher density of cross cutting dislocation channels and therefore an almost unaffected crack resistance. These explanations provide a rational to all experimental observations.


*PACS:* 61.80.Hg; 62.20.Mk; 81.40.Np; 81.70.Bt

## 1. Introduction

Neutron irradiation damage produced in structural materials is very often monitored using a tensile test. Such a test is quite easy and allows the determination of the material flow behavior. Examination of the tensile properties usually shows an increase of the yield strength and a reduction of ductility. At high fluence levels, the strain hardening capacity can drastically be reduced, resulting from localized deformation that occurs shortly after the yield strength is reached. This phenomenon, result of a heterogeneous plastic deformation that occurs in localized slip planes within bands of easy glide, is called dislocation channel deformation [1–4]. Indeed, in these bands, defect clearing by the initial unpinned dislocations provides paths of easy glide for subsequent dislocations, promoting therefore a localized plastic deformation. This phenomenon was observed in bcc, fcc and hcp metals [2,5–8]. A number of investigations are being devoted to this phenomenon [6–15], from both macroscopic and microscopic aspects, i.e., tensile testing and transmission electron microscopy (TEM), respectively. The mechanical response of a material experiencing plastic flow localization is characterized by a softening shortly after the yield strength. The TEM observations clearly show narrow defect-free channels or bands is which plastic deformation occurs preferentially [6,9,12,13,16–19]. Recently, a number of computer simulations including molecular dynamics were also reported to better understand this phenomenon [20–24]. However, to the author's knowledge, there was no attempt to investigate the plastic flow localization ahead of a crack tip. More specifically, the critical question is how this channel deformation mode will affect the fracture toughness behavior. It is, therefore, very interesting to examine the deformation and fracture mechanism in such high triaxial stress–strain fields

* Tel.: +49 2461 614683; fax: +49 2461 613699 (until September 2007).
*E-mail address:* r.chaouadi@fz-juelich.de
[1] On leave from SCK·CEN, Boeretang 200, 2400 Mol, Belgium. After September 2007, rchaouad@sckcen.be.

0022-3115/$ - see front matter © 2007 Elsevier B.V. All rights reserved.
doi:10.1016/j.jnucmat.2007.04.044

which are very different from those experienced during a standard tensile test.

## 2. Background

The present investigation was motivated by two considerations. First, there is a need of characterizing structural materials in their regime of operation conditions, namely at high temperature. Most irradiation studies directed towards irradiation effects on the mechanical properties concern the avoidance of the risk of brittle (catastrophic) failure. Therefore, the experimental data are usually reported in terms of ductile-to-brittle transition temperature (DBTT), either based on Charpy impact or fracture toughness data. However, the structural materials of the components are usually operated in a high temperature regime. Therefore, estimation of their crack resistance behavior is important in order to ensure adequate operation. Second, recent observations were reported on the disagreement between DBTT-shift as determined from Charpy impact tests in comparison to fracture toughness tests [25,26]. This disagreement could be explained in [27] by using the load diagram approach. Since part of the Charpy impact absorbed energy at the DBTT is spent in ductile fracture, it is important to understand how irradiation is affecting the flow and fracture behavior in the ductile regime. Therefore, the present work was initiated to provide better insight into the effect of plastic flow localization on the crack resistance behavior. More specifically, the subject of the present paper is the plastic flow localization induced by irradiation where dislocation channel deformation is the main deformation mechanism. Indeed, plastic instability can occur in a number of other conditions such as metals and alloys after quenching and subsequent heat treatment (ageing, tempering), predeformation or precipitation hardening [5,28]. However, the observation of a prompt necking after the yield strength that is usually observed on a tensile curve does not necessarily indicate a dislocation channel deformation mechanism. For example, at relatively high temperatures, plastic flow instability may occur without involving the dislocation channeling mechanism. This was observed in [26] for Eurofer-97 where plastic flow localization occurs above about 500 °C, but fracture toughness and crack resistance remain unaffected in comparison to room temperature. That's why it is preferred to define the phenomenon under investigation as irradiation-induced plastic flow localization involving specifically the dislocation channel deformation.

Before giving the experimental conditions, it is important to note that irradiation-induced plastic flow localization was long associated with low temperature embrittlement where typically a very significant hardening is observed when the irradiation temperature is below ~250 °C [7,8,29]. However, plastic strain localization is also found at higher irradiation temperature, 300 °C for example, although not as spectacular as observed in the low temperature range. In particular, the 9%Cr–1W ferritic/martensitic steel, Eurofer-97, was the subject of many investigations in Europe [26,30–38].

## 3. Experimental

The chemical composition of Eurofer-97 is given in Table 1. Some mechanical properties in the unirradiated condition are given in Table 2. Eurofer-97 was irradiated at SCK·CEN in the BR2 reactor at 300 °C up to about 2.1 dpa and was extensively characterized by Lucon [25,26,33] using tensile, Charpy impact and brittle fracture toughness tests. Because of the limited number of available specimens, the Charpy reconstitution technique was used to manufacture a few additional Charpy specimens from the broken ones. These were precracked to a crack length-to-width ratio close to 0.5 and further 20%-side grooved before testing at 300 °C in three-point bending at quasi-static loading.

The crack resistance curve was determined using the single specimen procedure based on the load–displacement test record. All specimens were tested using the unloading compliance method at 300 °C but the crack resistance curve determination was based on the load–displacement record according to a procedure detailed in [39]. After the crack has reached about 2.0 ± 0.5 mm crack extension, the specimens were unloaded, heat tinted (300 °C for 20 min), and further broken at low (liquid nitrogen)

Table 1
Chemical composition and heat treatment of Eurofer-97 (wt%)

| C | Ni | Cr | Mo | Cu | Si | Nb | V | P | Mn | W | Ta | Fe |
|---|---|---|---|---|---|---|---|---|---|---|---|---|
| 0.12 | 0.007 | 8.99 | <0.001 | 0.022 | 0.07 | <0.001 | 0.19 | <0.005 | 0.44 | 1.1 | 0.14 | Bal |

Table 2
Tensile (at 25 °C), impact and fracture properties of unirradiated Eurofer-97

| $\sigma_y$ (MPa) | $\sigma_u$ (MPa) | $\varepsilon_u$ (%) | $\varepsilon_t$ (%) | RA (%) | USE (J) | DBTT (°C) | $T_{100\,MPa\sqrt{m}}$ (°C) | $J_Q$ at 25 °C (kJ/m$^2$) |
|---|---|---|---|---|---|---|---|---|
| 557 | 670 | 5 | 20 | 80 | 251 | −57 | −115 | 300 |

$\sigma_y$ is the yield strength, $\sigma_u$ is the tensile strength, $\varepsilon_u$ is the uniform elongation, $\varepsilon_t$ is the total elongation, RA is the reduction of area, USE is the Charpy upper shelf energy, DBTT is the ductile-to-brittle transition temperature measured at 50% of the USE, $T_{100\,MPa\sqrt{m}}$ is the static fracture toughness transition temperature and $J_Q$ is the ductile initiation toughness evaluated at 0.2 mm crack extension.

temperature to better reveal the final crack front. The tests were performed according to the ASTM E-1820 testing procedure [40]. Note that although not in full agreement with the validity requirements according to the E-1820 standard, mainly in terms of specimen size, the results based on precracked Charpy specimens are believed to be valid and provide comparable results to large specimens, as demonstrated in [39].

## 4. Results and discussion

Before examining the fracture toughness results, it is interesting to show how the tensile curve is affected by neutron exposure.

### 4.1. Tensile test results

The tensile tests were taken from [26]. Fig. 1 shows the engineering stress–engineering plastic strain curves of Eurofer-97 irradiated at 300 °C to various dose levels and tested at 300 °C. As it can be seen, as neutron fluence increases a strong yield strength elevation together with a significant reduction of ductility are observed. Above about 1 dpa, plastic instability becomes evident, characterized by a premature necking occurring shortly after the yield strength is reached. This observation is typical of many materials experiencing dislocation channel deformation [6,9,12–15,29,41–47].

The occurrence of plastic flow localization was extensively investigated by Byun and co-workers [6–11,16–19]. By analyzing a number of materials, irradiation and testing conditions, they proposed a common stress criterion for plastic instability corresponding to the true stress at necking. This critical stress, defined as the plastic instability stress (PIS), is temperature dependent but remains unaffected by irradiation [6,8,47–49]. In Eurofer-97 at 300 °C, a PIS of ≈600 MPa is found. This is close to the yield strength at which flow localization is observed in Fig. 1 (≈635 MPa). However, this is not the case in all materials. In particular, ferritic steels irradiated at 265 °C up to ≈0.25 dpa indicate an increasing PIS with neutron exposure from 650 to 1070 MPa [50]. Also, contrary to what was reported in [48], it is believed that the mechanical behavior at, or after, the onset of necking is not the same for cold work and irradiation. The plastic flow instability that appears for a cold worked specimen is still homogeneous without dislocation channel deformation, while in an irradiated material this instability is resulting from a heterogeneous deformation resulting from the dislocation channel deformation [51,52].

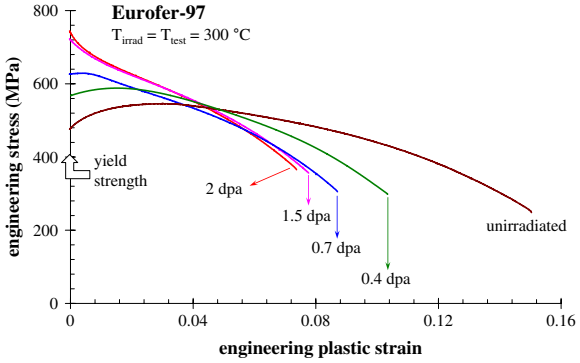


Fig. 1. Effect of irradiation on the flow curve at $T_{test} = 300$ °C [26].

### 4.2. Crack resistance test results at quasi-static loading rate

Although less critical than brittle fracture, the upper shelf behavior is also a parameter that is monitored to ensure safe operation of nuclear components. Indeed, over their normal operation life that occurs usually in the ductile regime, structural components should not fail. It is generally considered that the material should exhibit a good fracture resistance if the Charpy upper shelf energy level remains above a specific value. Upon irradiation, very often, a decrease of the upper shelf energy is observed indicating a loss of tearing resistance. However, the remaining crack resistance capacity is still high to avoid premature failure. It was reported in [25] that the decrease of the upper shelf energy level of Eurofer-97 is very small and therefore, its tearing resistance is assumed to be little affected. This was also observed on a number of other ferritic/martensitic steels [53]. As it will be seen later, this will not be the case.

While irradiation was found to have little effect on the Charpy impact test at the upper shelf level [25,26], the load–displacement test records indicate a drastic effect of irradiation, in particular by a drastic reduction of the deformation. Such test records provide a fingerprint of a drastic change of fracture resistance. Indeed, the crack resistance curves shown in Fig. 2 clearly show a tremendous loss of tearing resistance, in contradiction with the Charpy impact upper shelf data.

In Table 3, a number of parameters characterizing the ductile fracture resistance were summarized. Both initiation toughness and tearing resistance are affected. The significant change occurs between 0.35 and 1.26 dpa. Below

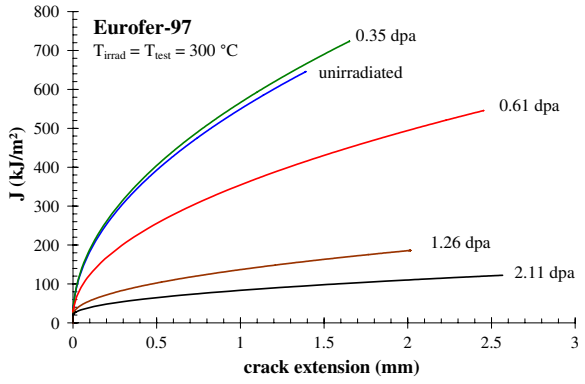


Fig. 2. Effect of irradiation on the crack resistance curve of Eurofer-97 at quasi-static loading rate.

Table 3
Crack resistance parameters of unirradiated and irradiated Eurofer-97 (quasi-static loading rate, ≈0.3 kJ m$^{-2}$ s$^{-1}$)

| Id | $T_{test}$ (°C) | Dose (dpa) | $J_{0.2}$ (kJ/m$^2$) | $J_Q$ (kJ/m$^2$) | $J_i$ (kJ/m$^2$) | $J_t$ (kJ/m$^2$ $\sqrt{}$mm) | $\Delta a_{end}$ (mm) |
|---|---|---|---|---|---|---|---|
| 0 | 300 | 0 | 254 | 342 | 13.8 | 536 | 1.39 |
| E97-07L | 300 | 0.35 | 262 | 340 | 14.8 | 552 | 1.65 |
| E97-62R | 300 | 0.61 | 169 | 196 | 18.4 | 338 | 2.45 |
| E97-15L | 300 | 1.26 | 74 | 77 | 21.3 | 117 | 2.02 |
| E97-39L | 300 | 2.11 | 50 | 51 | 21.1 | 64 | 2.57 |

$J_{0.2}$: $J$-value at 0.2 mm crack extension.
$J_Q$: $J$-value at 0.2 mm offset of the blunting line such as $J_{bl} = 4\sigma_f \Delta a$ (where $\sigma_f$ is the flow stress).
$J_i$: $J$-value at onset of ductile crack growth ($J = J_i + J_t\sqrt{\Delta a}$).
$J_t$: $J$-value characterizing the tearing resistance ($J = J_i + J_t\sqrt{\Delta a}$).
$\Delta a_{end}$: final ductile crack extension at the end of the test.

≈0.35 dpa, the effect of irradiation is negligible. Above ≈1 dpa, the degradation rate decreases. These effects are illustrated in Fig. 3 for both initiation toughness and tearing resistance. Note that the solid lines shown in Fig. 3 are not based on any model but are only trend curves. Similar trend curves were reported by Little [54] and Mills [55] on austenitic stainless steels, by de Vries on a martensitic steel [56], by Mills [57,58] on Inconel X-750 and Ni–Fe–Cr alloys and by Maloy et al. [59] on austenitic stainless steels, 9Cr–1Mo martensitic steel and Inconel 718.

The drastic decrease of crack resistance was not expected from the Charpy impact data. Differences stemming from notch acuity (V-notch versus crack tip) and loading rate effect could be suspected. Because of the limited availability of irradiated material, it was decided to examine first the loading rate effect by performing impact fracture toughness tests on precracked Charpy specimens. These tests are presented in the next subsection.

### 4.3. Crack resistance test results at dynamic loading rate

The procedure for crack resistance determination at impact loading is identical to quasi-static loading. Here, the reconstituted precracked Charpy sample is impact loaded on an instrumented Charpy impact machine. The Charpy impact hammer is positioned such that a fixed amount of energy, more precisely 30 J for the unirradiated material and 18 J and 20 J in the irradiated condition, is available for crack extension. The load–time trace is transformed to a load–displacement curve and further used to calculate the $J$-integral. Using the measured specimen dimensions, fatigue crack length and ductile crack extension, the crack resistance curve can accurately be determined. Note that the $J$-rate at quasi-static loading corresponds roughly to about 0.3 kJ m$^{-2}$ s$^{-1}$ while at the dynamic loading rate it corresponds to about $3 \times 10^5$ kJ m$^{-2}$ s$^{-1}$.

The quasi-static and dynamic crack resistance curves are compared in Fig. 4 for two specimens reconstituted from the same original Charpy impact sample ($\Phi = 0.61$ dpa). There is a clear difference between the two curves that cannot be attributed to a statistical scatter. Another irradiated precracked Charpy specimen with an accumulated dose of 1.33 dpa tested at room temperature exhibited a significantly higher crack resistance than under static loading. The effect of irradiation on the dynamic crack resistance is shown in Fig. 5 for the two test temperatures, 25 °C and 300 °C. Considering the inherent experimental scatter (±15%), it can be stated that no significant difference could be identified between the unirradiated and irradiated condition. The parameters characterizing the initiation and tearing resistance are summarized in Table 4. This clearly supports the Charpy impact data that exhibited a very little decrease of upper shelf energy upon irradiation. The notch acuity effect can be excluded and it is expected that

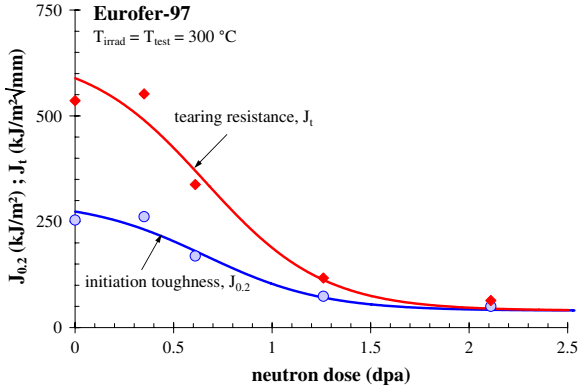


Fig. 3. Effect of irradiation on the initiation toughness, $J_{0.2}$ and tearing resistance, $J_t$.

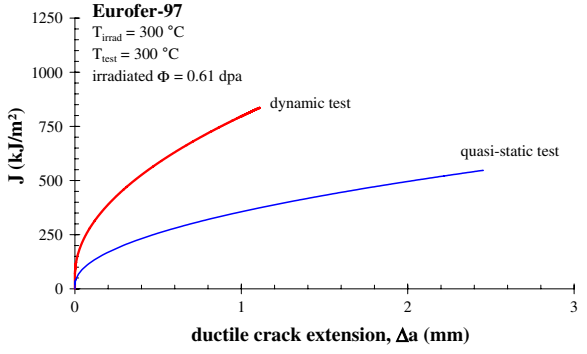


Fig. 4. Comparison of crack resistance behavior: quasi-static versus dynamic (impact) loading.

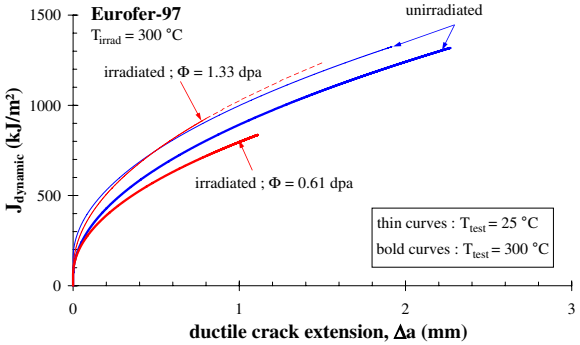


Fig. 5. Comparison of crack resistance behavior at dynamic (impact) loading.

V-notched Charpy tests at static loading would exhibit significantly lower absorbed energy than the impact loaded ones. The decrease of fracture toughness resistance with decreasing loading rate was also observed by de Vries [60] on an irradiated stainless type 304 steel and was attributed to a change of fracture mode from dimple to intergranular. However, in our case, as it will be shown in the next section, the fracture mechanism remains ductile.

While the consistency between Charpy impact data and dynamic crack resistance results is clearly established, the question arises why quasi-static loading shows a drastic degradation of crack resistance while no effect is observed at dynamic loading rate. Before attempting a reasonable explanation, it is necessary to first understand the reasons of such degradation at quasi-static loading. Indeed, the first question that comes out is: Are the fracture mechanisms similar? To answer this question, examination of the fracture surfaces was carried out using a scanning electron microscope to better reveal the underlying fracture mechanisms.

## 5. Scanning electron microscopy examination of the fracture surfaces

The precracked Charpy specimens used for crack resistance measurements were examined by scanning electron microscopy. First, all specimens examined show a typical dimple fracture surface, characteristic of ductile fracture. This clearly excludes any change of fracture mode with irradiation; in particular intergranular fracture does not occur. An example is shown in Fig. 6 where two fracture surfaces from an unirradiated and an irradiated (1.26 dpa) specimen tested in quasi-static loading rate are compared. Although not quantitatively and systematically investigated, the average dimple size decreases with irradiation. Another observation can be made on the dimple morphology. In the unirradiated condition, equiaxed dimples are observed while they become shallower after irradiation, probably as a result of shear deformation [61]. The main difficulty for a quantitative characterization of the dimple structure is that the fracture surface is not flat but rather rough, a zigzag kind of fracture (see Fig. 7(b)). The tendency to zigzag fracture increases with increasing neutron exposure. As a matter of fact, while ductile crack

Table 4
Crack resistance parameters of unirradiated and irradiated Eurofer-97 at dynamic loading rate ($\approx 3 \times 10^5$ kJ m$^{-2}$ s$^{-1}$)

| Id | $T_{test}$ (°C) | dose (dpa) | $J_{0.2}$ (kJ/m$^2$) | $J_Q$ (kJ/m$^2$) | $J_i$ (kJ/m$^2$) | $J_t$ (kJ/m$^2$ $\sqrt{}$mm) | $\Delta a_{end}$ (mm) |
|---|---|---|---|---|---|---|---|
| E97-116L | 25 | 0 | 523 | 671 | 140 | 856 | 1.92 |
| E97-116R | 300 | 0 | 428 | 556 | 52 | 841 | 2.27 |
| E97-59L | 25 | 1.33 | 506 | 676 | 86 | 940 | 0.78 |
| E97-62L | 300 | 0.61 | 389 | 462 | 60 | 736 | 1.11 |

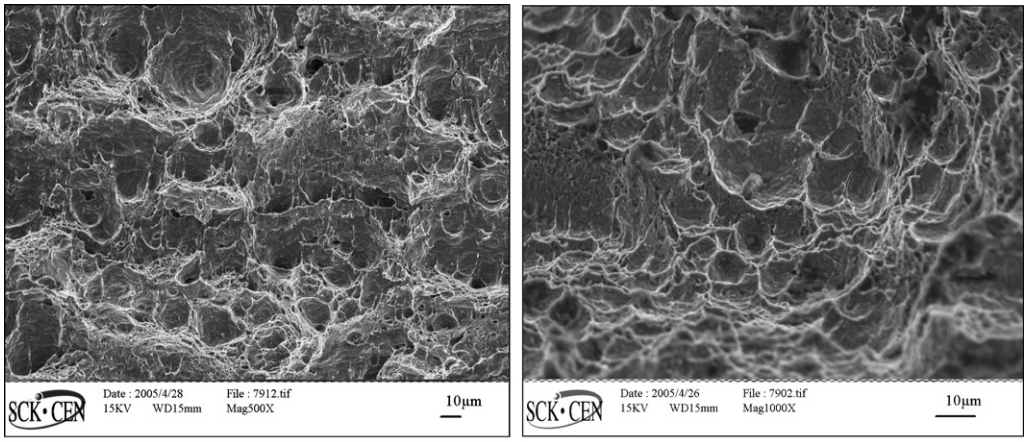


(a) 0 dpa (b) 1.26 dpa

Fig. 6. SEM fractography of the fracture surfaces exhibiting typical dimple fracture. Observation of equiaxed dimples (a) and combination of equiaxed and shear dimples (b).

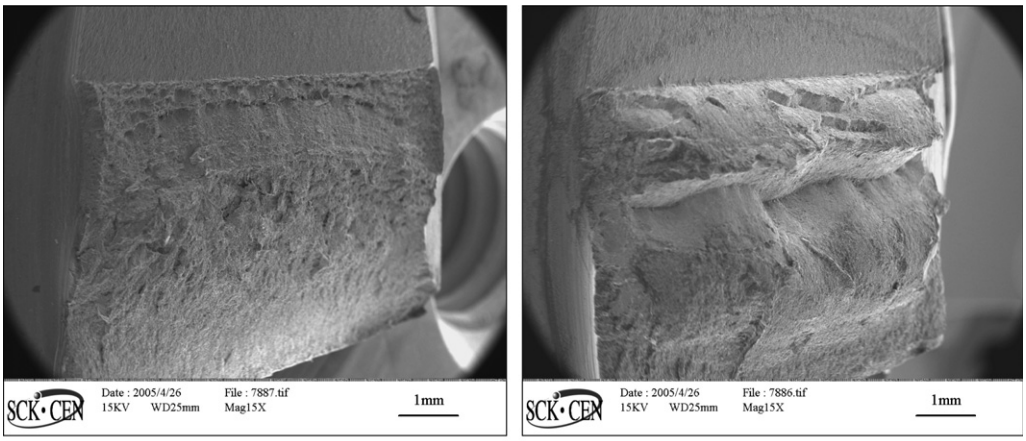


(a) 0.35 dpa (b) 2.11 dpa

Fig. 7. SEM fractography illustrating the zigzag fracture along specific planes characteristic of flow localization ($\Phi = 2.11$ dpa). The different crack zigzags are ~45°-oriented with respect to the fatigue precrack plane.

extension occurs on the plane of the fatigue precrack normal to the applied stress (quasi-flat surface) in the unirradiated and low dose irradiated samples, the fracture path exhibits a more accidental profile involving cracking along alternating shear planes [61]. The fracture surfaces are shown in Fig. 7 for two specimens irradiated to 0.35 and 2.11 dpa; the specimens were slightly tilted to better reveal their topography. As can be seen, these two pictures differ mainly in the path of the crack extension. Above a certain neutron dose level, say 0.5 dpa, step-like edges appear on the fracture surface corresponding to an abrupt change of the crack propagation direction. It is likely that this change of fracture topography coincides with the onset of plastic instability resulting from the occurrence of dislocation channel deformation. This suggests a direct relationship between crack resistance behavior and dislocation channel deformation. Note also that the different crack zigzags in Fig. 7(b) are ≈45°-oriented with respect to the fatigue precrack plane. So, one can suspect that the drastic decrease of crack resistance with neutron irradiation can be attributed to the change of fracture aspect from equiaxed to shear dimples. This correlation between fracture mode and crack resistance will be re-examined in the next section.

Note that in Fig. 7, the lower part of the fracture surface is cleavage; the actual crack extension from the initial fatigue crack front is given in Tables 3 and 4. These crack length measurements were performed using an optical microscope ignoring the sinuous aspect of the fracture surface, e.g. shown in Fig. 7(b). Nevertheless, although this aspect is not considered, the decrease of crack resistance is still very severe.

Finally, examination of the irradiated impact-tested specimens exhibits an equiaxed dimple fracture mode, similar to the unirradiated fracture surface. The reasons of such a difference in behavior with loading rate will be examined in the next section. At this stage, one can state that, as shown in Fig. 8 for the two samples reconstituted from the same Charpy specimen irradiated to 0.61 dpa, the ductile crack extension topographies ahead of the fatigue precrack differ significantly from one another.

## 6. Data analysis and interpretation

The preceding experimental observations, including both crack resistance results and SEM examination, can be summarized according to the following main question, namely, why, upon irradiation, the $J$–$R$ curve drastically

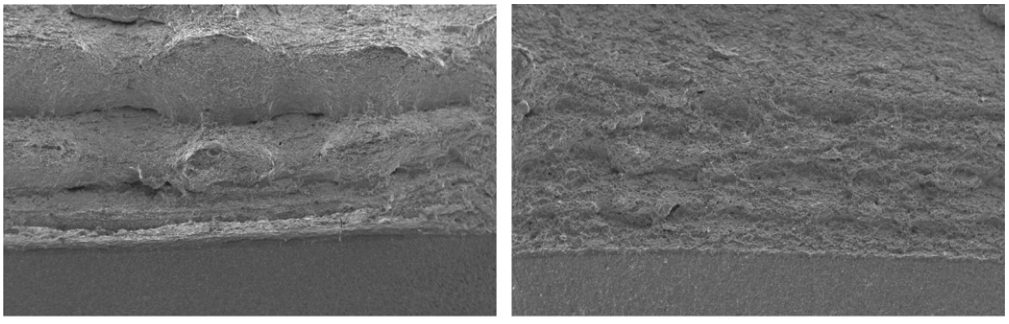

(a) static (heterogeneous shear) (b) dynamic (homogeneous shear)

Fig. 8. SEM fractography illustrating the effect of loading rate on the fracture ($\Phi = 0.61$ dpa).

decreases at quasi-static loading but remains almost unaffected at dynamic loading rate?

In the previous section, the SEM observations have revealed a change of crack extension topography of the quasi-statically tested specimens occurring when the deformation mode turns into a dislocation channel mode of deformation. This means that one can suspect the existence of a close relationship between the flow localization observed on the tensile curves and the reduction of fracture toughness and tearing resistance.

For the material investigated here, unfortunately, no TEM examination was carried out to clearly establish the occurrence of dislocation channel deformation after irradiation above ≈0.5 dpa. However, such observations were already made on a similar 9%Cr martensitic steel, F82H, irradiated at 300 °C [14,15]. Therefore, the same phenomenon is assumed to occur for the Eurofer-97 examined here, supported by the tensile curves shown in Fig. 1. As already mentioned, the main reason of irradiation-induced plastic strain localization is attributed to the defect clusters removal by dislocations moving in channels which delimit the principal slip planes [1–3]. High stresses are usually required to induce this phenomenon. The irradiation defects acting as obstacles to dislocation motion will allow reaching of the critical stress at which the pinned dislocations are suddenly unpinned. In their motion, the latter will remove most of the defects and consequently make the passage in the channel easier to subsequent dislocations. By such a process, the material becomes inhomogeneous, i.e., a composite material with defects-free layers (soft material) surrounded by a material containing defects (hard – as irradiated material) and the deformation is concentrated in these narrow channels [62]. Computer simulations, using dislocation dynamics, were also successfully used to help understanding the underlying fundamental mechanism of irradiation-induced localized deformation [22,24,63]. In particular, the mechanism of channel formation was found to be associated with dislocation pinning by the irradiation defect clusters (staking-fault tetrahedrons and Frank interstitial loops), followed by their unpinning as a result of defect absorption by the dislocations and their cross slip with increasing stress.

Most if not all of the experimental observations reported in literature concern specimens quasi-statically loaded in tension with relatively low stress triaxiality. Ahead of a crack tip, with significantly higher stress triaxiality, it is assumed that the same phenomenon would occur, namely the plastic deformation will be concentrated in narrow channels. It is known that the crack extension process occurring according to the microvoid nucleation, growth and coalescence mechanism is governed by plastic strain and stress triaxiality. However, in a heterogeneous material, hard with soft channels (see Fig. 9 for illustration), the plastic deformation is not homogeneous. As a result, the interface between these channels and the hard (as-irradiated) material offers a crack extension path requiring a minimum of energy. Indeed, as illustrated in

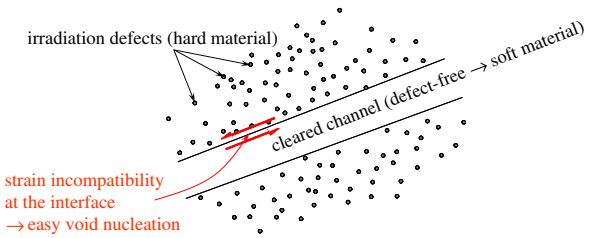


Fig. 9. Illustration of the fracture path along cleared channels interface.

Fig. 9, because of material deformation incompatibility at the interface, crack nucleation at the interface is promoted, facilitating the passage of a crack due to an easy void nucleation at intersecting slip bands [64]. This can reasonably explain the drastic degradation of the crack resistance when channel deformation mode occurs. This is also supported by the SEM observations that indicate crack extension following a sinuous path. The step-like edges observed on the fracture surface of Fig. 7(b) can be attributed to the intersection of the dislocation channel bands. Indeed, TEM observations on a number of materials indicate such intersections, or channel networks [16,49]. This explanation is also supported by a number of experimental observations on fracture at interfaces or mismatched materials. Indeed, the dislocation channel can be assimilated to a narrow interface. In literature, most of the reported measurements indicate a channel width of the order of 100–200 nm and a channel spacing in the range of 1–3 μm [4,17,65]. The spacing between channels was also reported to decrease with increasing strain. The channel width was found to be independent of the strain rate [4]. However, the strain rate range that was considered in [4], i.e., $10^{-5}$–$10^{-3}$ $s^{-1}$, was much smaller than what is considered in the present tests (several orders of magnitude higher, $10^{-4}$–$10^{+1}$ $s^{-1}$). Li and Guo [66] performed detailed finite element calculations to investigate the void growth and coalescence on a bi-material interface. Their results indicate that plasticity mismatch significantly affects the growth rate and coalescence strain of voids in bi-material interfaces. As a result, the growth rate of voids at the interface is much higher than in a homogeneous material. Another interesting investigation was performed by Tschegg et al. [67] by testing a bi-material, ferrite–austenite.

The crack resistance curve was found to significantly decrease when the crack is very close to the interface. Although not directly related to the dislocation channel deformation, these results clearly support the fact that the observed severe crack resistance degradation can be rationalized in terms of crack extension in a highly heterogeneous (interface-like) material.

The rational outlined above to explain the experimental observations, namely the severe degradation of crack resistance cannot be considered complete if the loading rate effects are not explained. It was shown in Fig. 4 that the crack resistance increases with loading rate. By contrast, Fig. 5 indicates obviously that the dynamic crack resistance remains unaffected by irradiation. This raises the question

if the loading rate has an effect on the development of fracture under plastic strain localization?

It is known that the crack resistance is increased by the loading rate [68–72]. This elevation of crack resistance can be explained by the state of local stress–strain conditions prevailing ahead of the crack tip. Detailed finite element calculations performed by Koppenhoefer and Dodds [73,74] clearly show that the increase of tearing resistance can be associated with a loss of constraint, or loss of triaxiality, that occurs at dynamic loading rates. Narasimhan and co-workers [75–78] also performed detailed numerical investigations on this issue. The elevated stresses at the crack tip generate high stresses in the remaining ligament leading to a greater plastic work elsewhere in the specimen. This so-called background plasticity is higher under dynamic than under static loading rate, and therefore requires additional work to fracture resulting in an extended plastic zone size ahead of the crack tip. In our situation, at static loading rates, the dislocation channel deformation is limited to a small zone ahead of the crack tip where the fracture path is facilitated by the near presence of a heterogeneous soft/hard interface where microvoids can easily nucleate. Indeed, because of plastic strain incompatibility induced by large stress concentrations at the interface between the channel and the unaffected matrix material, formation of small voids occurs, thus destroying the continuity of the matrix and degrading its bearing ability. At dynamic loading rates, this zone is extended such as a large part of the material ahead of the crack tip is softened by the dislocation channeling process, increasing thereby the tearing resistance. Indeed, at impact loading, the strain rate ahead of the crack tip can reach very high values, typically in the order of $10^3$–$10^4$ $s^{-1}$ [73,79–84]. This leads to an increase of local temperature (adiabatic process) that might promote annealing of the irradiation defects [2]. During high strain rate deformation, a significant increase of the effective temperature is usually expected as a result of intense heating due to the dissipation of plastic deformation work [85–87]. Due to experimental difficulties for measuring temperature at the crack tip during a very short duration, there are not many reported quantitative data on temperature elevation. However, temperature increases in the range 100–1000 K were reported in literature [86,88,89]. Rossoll et al. [81] reported a temperature increase at the notch root of a Charpy impact specimen of more than 200 K. Theoretical simulations predict very high temperatures of the order of a few hundreds, that increase with strain up to above 1000 K [86,87]. However, given the short time duration over which such a temperature increase may occur, it is believed that this is not enough to induce locally a full thermal recovery leading to an unchanged crack resistance behavior.

Another mechanism, the so-called dislocation-free deformation mechanism introduced by Kiritani and coworkers [90–94] and occurring at very high strain rates – typically above about $10^3$ $s^{-1}$ – is examined. This was related to the formation of a high density of point defect clusters, more specifically vacancy clusters [93], that occurs at high strain rates. The plastic deformation proceeds then by a simultaneous shift of positions of many atoms, without involving dislocations. However, this is not supported by the computer simulations performed by Schiotz et al. [95,96] despite the confirmation of the high vacancy concentrations experimentally observed by Kiritani et al. [90]. The non-observation of dislocations was explained by the formation of a dislocation-free zone close to the crack tip [95]. So, the plastic deformation is believed to occur according to the classical dislocation mechanism. The deformation mechanism was reported to change, around $10^3$ $s^{-1}$, from a heterogeneously distributed group of dislocations to a random distribution [93]. Indeed, at low strain rates, glide dislocations are stopped by other dislocations leading to the development of a dislocation cell structure. At much higher strain rates, dislocations are considered to be stopped by obstacles other than dislocations, most probably vacancy clusters, leading to a random distribution [93]. In this mode of deformation, plastic deformation seems to occur uniformly in the matrix by the simultaneous sliding of numerous planes rather than by localized slide motion of dislocation [92]. All these descriptions reported in literature are consistent with the present experimental observations.

Because higher peak stresses are reached in a larger plastic (process) zone, more dislocation sources will be activated. As a result, the defect clearing mechanism observed inside the channels would occur in a larger volume when the loading rate is increased. This will induce a more dense dislocation channeling activity and consequently a larger volume of defect-free material in which ductile fracture occurs in a homogeneous manner by the classical microvoid coalescence process similar to the unirradiated material.

It is also likely that the mode of failure changes from the classical opening mode I to a mixed mode I–II when decreasing loading rate from dynamic (impact) to quasistatic. This is illustrated in Fig. 10 which shows the interaction of a crack tip with a dislocation channel. It is known that mode mixity, for example I–II or I–III, decreases the fracture resistance in comparison to mode I alone [97–100]. Hence, under predominant mode II loading, the *J*-integral value is reduced because of the localization of plastic deformation into a narrow band ahead of the crack tip [98]. Indeed, the reduction of the hydrostatic stress component has an important implication on the void growth and failure of the ligament by microvoid coalescence [97,101]. In mode I (opening loading mode) high stress triaxiality promotes void growth and fracture occurring by void link-up through necking of the inter-void ligaments until impingement. In mode II (shear loading mode), voids experience limited void growth due to low stress triaxiality and final link-up between voids occurs through shear localization of plastic strain in the ligaments between voids. The SEM micrographs shown in Figs. 6(b) and 7(b) support such a fracture mode. However, in the present case, the

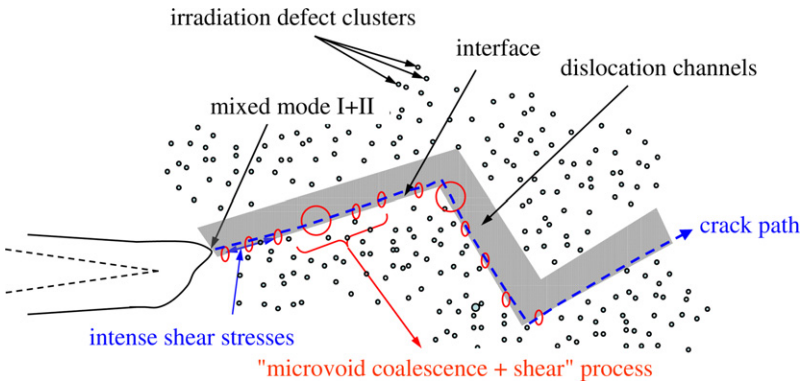


Fig. 10. Illustration of the local crack tip conditions promoting the crack propagation along interface.

profile of the crack path is accidental rather than propagating at a constant angle with respect to the crack plane in a homogeneous material because the dislocation channel bands are arbitrary oriented according to specific slip planes [102,103]. This explanation contributes also to understand the fracture behavior of the irradiated material under both static and dynamic loading rates.

It was already mentioned that the upper shelf energy was essentially unaffected by irradiation. In Fig. 11, the load–time test record of an unirradiated Charpy sample is compared to the irradiated one (time is put in a logarithmic scale to better illustrate the similarities and differences). Both specimens exhibit a typical ductile fracture in the upper shelf regime. As it can be seen, both curves are quasi-similar, in particular in the tearing part. The main difference is essentially located in the initiation part below ~1 ms. Fig. 11 clearly suggests that the initial phase of crack initiation – below 1 ms – in the irradiated material, modifies the material ahead of the notch/crack and that further crack propagation occurs in both unirradiated and irradiated material in a very similar way. This clearly indicates that testing modifies the material properties.

Finally, it is important to outline some possible consequences of such a behavior, namely the change of fracture mechanism with irradiation and loading rate. Although the work presented here is based on a 9%Cr tempered martensitic steel, it does not exclude its occurrence in other materials including ferritic steels. It is therefore important to carefully examine Charpy impact data of materials where flow localization occurs. As a matter of fact, high fluence irradiation promotes such a phenomenon. Also heterogeneous materials such as a heat affected zone (HAZ) of pressure vessel steels should be carefully examined. Under certain circumstances, it is possible that the HAZ can offer a preferential path for fracture propagation at quasi-static loading rate although the Charpy impact tests will not indicate effects of irradiation. There is also an important topic related to specimen size. For a long time, there was a tendency to miniaturize test specimens that are used to evaluate the mechanical properties of fusion materials [104–113]. Indeed, it is known that in the case of the International Fusion Materials Irradiation Facility (IFMIF), the high flux irradiation region will not exceed 0.5 l [114–117]. To rationalize the available irradiation space, the use of miniature specimens is obvious. However, the use of small samples may induce a loss of constraint that can locally modify the structure and lead to apparent high toughness. There was also much attention paid to the small punch test and many correlations were established between the DBTT measured from Charpy impact data and small punch tests [118–129]. However, as shown in this work, these correlations might be biased by the loading rate. It is important to make sure that the deformation and fracture mechanisms are not affected by using small specimens that experience significant loss of constraint.

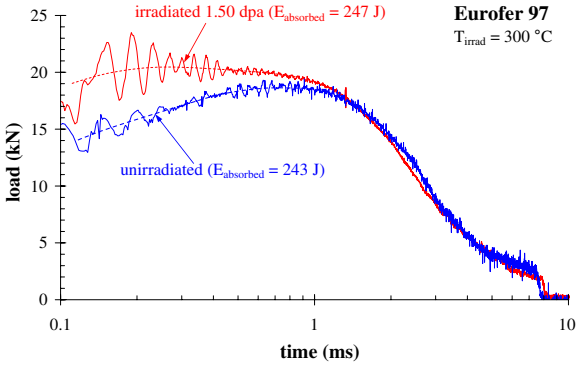


Fig. 11. Comparison of load–time records of Charpy impact tests at upper shelf upon irradiation.

## 7. Summary and conclusions

The work presented in this paper clearly demonstrates the importance of combining various mechanical properties together with different microstructural observations to unambiguously characterize and understand the material behavior under irradiation. It is shown that in presence of irradiation-induced plastic instability, the crack resistance of the material is severely reduced under static loading but not under dynamic (impact) loading. This is the reason why the DBTT-shift measured using Charpy impact data was systematically found smaller than the fracture toughness transition temperature shift.

Two important questions were raised by the experimental results presented in this work. First, why does the crack resistance curve drastically decrease upon irradiation under static loading? The second question is why at dynamic (impact) loading rate, the crack resistance remains unaffected by irradiation?

For both questions, the answer is intimately related to fracture micro-processes that develop ahead of the crack tip, in particular the flow localization resulting from dislocation channel deformation.

Under static loading, because of the occurrence of dislocation channel deformation, the material becomes inhomogeneous and ahead of the crack tip, it behaves like an interface. Consequently, because of the deformation incompatibility at the interface between the defect-free channels and the surrounding as-irradiated material, void initiation is promoted offering therefore an easy crack propagation path. Moreover, since the dislocation channels are arbitrarily orientated, a mixed (I + II) mode rather that mode I fracture will dominate ahead of the crack tip. It is the mixed mode (I + II) ahead of an interface material that is primarily responsible for the drastic degradation of the static crack resistance.

However, under dynamic (impact) loading, there are two additional phenomena that should be considered. Firstly, the inertial effects induce locally adiabatic heating, therefore an increase of the local temperature that promotes the recovery of the material properties. Secondly, the inertial effects induce high peak stresses and therefore high plastic zones ahead of the crack tip, which induce a significant loss of constraint. As a result, a higher density of dislocation channel bands may develop because more dislocation sources are activated. As a result of the combination of high local temperatures and material volume which is free of defects, the material ahead of the crack tip behaves such as the unirradiated material.

The explanations provided in this paper offer a rational to all the experimental observations carried out in this work, including tensile, Charpy impact, fracture toughness and crack resistance properties and scanning electron microscopy of the fracture surfaces. They are also supported by a number of studies found in literature such as the fracture behavior of interface (or bi-)materials and fracture under mixed mode. In this respect, heterogeneous materials such as irradiated heat affected zones should be carefully examined to avoid preferential crack propagation along the interface.

Finally, it is essential to emphasize the importance of the loading history on the fracture mechanisms. In particular, it was shown that Charpy impact data can experience a significant loss of constraint to induce recovery of the fracture properties. By extension, attention should be paid when examining fracture toughness test data using quasi-statically loaded miniaturized specimens. Indeed, a loss of constraint is promoted by the reduction of the specimen size that can locally modify the structure and lead to apparent high toughness.

## Acknowledgements

This work presented in this paper, supported by the Fusion European Program, was performed at SCK·CEN (mainly the experimental work and the data analysis and interpretation) within the Underlying Technology task UT-MOD-2005 and at Forschungszentrum Jülich (results interpretation and discussion) within the Helena project. The author is indebted to M. Decréton and E. Lucon for the strong support they provided to perform this work. Special gratitude is expressed to R. Mertens for specimen fabrication, to L. Van Houdt for testing and to A. Leenaers for SEM examination. Many thanks to J. Linke, T. Hirai and G. Pintsuk of the Fusion Materials group of Forschungszentrum Juelich for the fruitful discussions and the reviewing of this paper.

## References

[1] A.L. Bement Jr., Second International Conference on the Strength of Metals and Alloys, vol. 3, The American Society for Metals, 1970, p. 693.
[2] M.S. Wechsler, The Inhomogeneity of Plastic Deformation, American Society for Metals, Metals Park, OH, 1971, p. 19.
[3] R.P. Tucker, M.S. Wechsler, S.M. Ohr, J. Appl. Phys. 40 (1969) 400.
[4] J.V. Sharp, Philos. Mag. 16 (1967) 77.
[5] A. Luft, Prog. Mater. Sci. 35 (1991) 97.
[6] T.S. Byun, K. Farrell, N. Nashimoto, J. Nucl. Mater. 329–333 (2004) 998.
[7] T.S. Byun, K. Farrell, J. Nucl. Mater. 326 (2004) 86.
[8] T.S. Byun, K. Farrell, Acta Mater. 52 (2004) 1597.
[9] K. Farrell, T.S. Byun, N. Hashimoto, J. Nucl. Mater. 335 (2004) 471.
[10] K. Farrell, T.S. Byun, J. Nucl. Mater. 318 (2003) 274.
[11] K. Farrell, S.T. Mahmood, R.E. Stoller, L.K. Mansur, J. Nucl. Mater. 210 (1994) 268.
[12] D.J. Edwards, B.N. Singh, J.B. Bilde-Sorensen, J. Nucl. Mater. 342 (2005) 164.
[13] B.N. Singh, N.M. Ghoneim, H. Trinkaus, J. Nucl. Mater 307–311 (2002) 159.
[14] N. Hashimoto, S.J. Zinkle, R.L. Klueh, A.F. Rowcliffe, K. Shiba, Mater. Res. Soc. Symp. Proc. 650 (2001) R1.10.1.
[15] N. Hashimoto, R.L. Klueh, M. Ando, H. Tinigawa, T. Sawai, K. Shiba, Fus. Sci. Technol. 44 (2003) 490.
[16] T.S. Byun, N. Hashimoto, K. Farrell, E.H. Lee, J. Nucl. Mater. 349 (2006) 251.
[17] N. Hashimoto, T.S. Byun, K. Farrell, S.T. Zinkle, J. Nucl. Mater. 336 (2005) 225.
[18] N. Hashimoto, T.S. Byun, K. Farrell, S.T. Zinkle, J. Nucl. Mater. 329–333 (2004) 947.
[19] E.H. Lee, T.S. Byun, D.J. Hunn, K. Farrell, L.K. Mansur, J. Nucl. Mater. 296 (2001) 183.
[20] Y. Yang, N. Sekimura, H. Abe, J. Nucl. Mater. 329–333 (2004) 1208.
[21] J.S. Robach, I.M. Robertson, B.D. Wirth, A. Arsenlis, Philos. Mag. 83 (2003) 955.
[22] T.A. Khraishi, H.M. Zbib, T.D. de la Rubia, M. Victoria, Metall. Mater. Trans. 33B (2002) 285.
[23] L.Z. Sun, N.M. Ghoneim, S.H. Tong, B.N. Singh, J. Nucl. Mater. 283–287 (2000) 741.
[24] T.D. de la Rubia, H.M. Zbib, T.A. Khraishi, B.D. Wirth, M. Victoria, M.J. Caturla, Nature 406 (2000) 871.
[25] E. Lucon, J. Nucl. Mater. 329–333 (2004) 1078.

[26] E. Lucon, Mechanical properties of the European reference RAFM steel (EUROFER-97) before and after irradiation at 300 °C (0.3–2 dpa), SCK·CEN report BLG-962, 2003.
[27] R. Chaouadi, J. Nucl. Mater. 360 (2007) 75.
[28] B. Brenner, A. Luft, Mater. Sci. Eng. 52 (1982) 229.
[29] J.E. Pawel, A.F. Rowcliffe, D.J. Alexander, M.L. Grossbeck, K. Shiba, J. Nucl. Mater. 233–237 (1996) 202.
[30] J. Rensman, H.E. Hofmans, E.W. Schuring, J. van Hoepen, J.B.M. Bakker, R. den Boef, F.P. van den Broek, E.D.L. van Essen, J. Nucl. Mater. 307–311 (2002) 250.
[31] J. Rensman, E. Lucon, J. Boskeljon, J.V. Hoepen, R. Den Boef, P. Ten Pierick, J. Nucl. Mater. 329–333 (2004) 1113.
[32] B. van der Schaaf, F. Tavassoli, C. Fazio, E. Rigal, E. Diegele, R. Lindau, G. LeMarois, Fus. Eng. Des. 69 (2003) 197.
[33] E. Lucon, Characterization of the mechanical properties of EUROFER in the unirradiated and irradiated condition, SCK·CEN report BLG-945, 2003.
[34] R. Andreani, E. Diegele, R. Laesser, B. van der Schaaf, J. Nucl. Mater. 329–333 (2004) 20.
[35] P. Fernandez, A.M. Lancha, J. Lapena, M. Hernandez-Mayoral, Fus. Eng. Des. 58–59 (2001) 787.
[36] R. Lindau, M. Schirra, Fus. Eng. Des. 58–59 (2001) 781.
[37] R. Lindau, A. Möslang, M. Schirra, Fus. Eng. Des. 61&62 (2002) 659.
[38] P. Spätig, G.R. Odette, G.E. Lucas, M. Victoria, J. Nucl. Mater. 307–311 (2002) 536.
[39] R. Chaouadi, J. Test. Eval. 32 (2004) 469.
[40] E 1820-01, Standard Test Method for Measurement of Fracture Toughness, Annual Book of ASTM Standards, Section 3, Metals Test Methods and Analytical Procedures, vol. 03.01, American Society for Testing and Materials, 2002.
[41] X. Wu, X. Pan, M. Li, J.F. Stubbins, J. Nucl. Mater. 343 (2005) 302.
[42] K. Farrell, T.S. Byun, N. Hashimoto, Mapping flow localization processes in deformation of irradiated reactor structural alloys – Final report, ORNL/TM-2003/63, 2003.
[43] S.A. Maloy, M.R. James, W.R. Johnson, T.S. Byun, K. Farrell, M.B. Toloczko, J. Nucl. Mater. 318 (2003) 283.
[44] N. Hashimoto, S.J. Zinkle, A.F. Rowcliffe, J.P. Robertson, S. Jitsukawa, J. Nucl. Mater. 283–287 (2000) 528.
[45] A.F. Rowcliffe, J.P. Robertson, R.L. Klueh, K. Shiba, D.J. Alexander, M.L. Grossbeck, S. Jitsukawa, J. Nucl. Mater. 258–263 (1998) 1275.
[46] T. Onchi, J. Nucl. Mater. 88 (1980) 226.
[47] T.S. Byun, K. Farrell, E.H. Lee, J.D. Hunn, L.K. Mansur, J. Nucl. Mater. 298 (2001) 269.
[48] T.S. Byun, N. Hashimoto, K. Farrell, Acta Mater. 52 (2004) 3889.
[49] T.S. Byun, N. Hashimoto, K. Farrell, J. Nucl. Mater. 351 (2006) 303.
[50] R. Chaouadi, An engineering radiation hardening model for RPV materials, SCK·CEN report R-4235, 2005.
[51] A. Korbel, P. Martin, Acta Metall. 36 (1988) 2575.
[52] R.L. Fish, J.L. Straalsund, C.W. Hunter, J.J. Holmes, in: Effects of Radiation on Substructure and Mechanical Properties of Metals and AlloysASTM STP, 529, ASTM, 1973, p. 149.
[53] E. Lucon, A. Almazouzi, Mechanical response to irradiation at 200 °C for EM10, T91 and HT9 steels – Final Report: Specimen irradiated to 2.6 and 3.9 dpa, SCK·CEN report BLG-986, 2004.
[54] E.A. Little, J. Nucl. Mater. 139 (1986) 261.
[55] W.J. Mills, Nucl. Technol. 82 (1988) 290.
[56] M.I. de Vries, in: A.S. Kumar et al. (Eds.), Effects of Radiation on Materials: 16th International Symposium, ASTM STP, vol. 1175, ASTM, 1993, p. 558.
[57] W.J. Mills, Eng. Fract. Mech. 18 (1983) 601.
[58] W.J. Mills, Eng. Fract. Mech. 26 (1987) 223.
[59] S.A. Maloy, M.R. James, G. Willcutt, W.F. Sommer, M. Sokolov, L.L. Snead, M.L. Hamilton, F. Garner, J. Nucl. Mater. 296 (2001) 119.
[60] M.I. de Vries, in: F.A. Garner et al. (Eds.), Influence of Radiation on Material Properties: 13th International Symposium (Part II), ASTM STP, 956, ASTM, 1987, p. 162.
[61] C.D. Beachem, G.R. Yoder, Metall. Trans. 4 (1973) 1145.
[62] B.N. Singh, A.J.E. Foreman, H. Trinkaus, J. Nucl. Mater. 249 (1997) 103.
[63] D. Rodney, Nucl. Instrum. and Meth. B 228 (2005) 100.
[64] A. Gysler, G. Lutjering, V. Gerold, Acta Metall. 22 (1974) 901.
[65] Z. Yao, R. Schäublin, M. Victoria, J. Nucl. Mater. 307–311 (2002) 374.
[66] Z. Li, W. Guo, Int. J. Plast. 18 (2002) 249.
[67] E. Tschegg, H.O.K. Kirchner, M. Kocak, Acta Metall. Mater. 38 (1990) 469.
[68] W.L. Server, in: J.D. Landes et al. (Eds.), Elastic–Plastic Fracture, ASTM STP, 668, ASTM, 1979, p. 493.
[69] D.A. Curry, I. Milne, R.S. Gates, Mater. Sci. Eng. 63 (1984) 101.
[70] K. Brünighaus, W. Hesse, M. Twinckler, R. Twinckler, W. Dahl, J. Phys., Colloque C5 supplément au no 8 46 (1985) C5-225.
[71] T. Kobayashi, S. Yamada, Metall. Mater. Trans. 25A (1994) 2427.
[72] R. Chaouadi, J.L. Puzzolante, Fatigue Fract. Engng. Mater. Struct., in press.
[73] K.C. Koppenhoefer, R.H. Dodds, Nucl. Eng. Des. 180 (1998) 221.
[74] K.C. Koppenhoefer, R.H. Dodds, in: Fatigue and Fracture Mechanics: 29th Volume, ASTM STP, 1332, ASTM, 1999, p. 135.
[75] P. Biswas, R. Narasimhan, Mech. Mater. 45 (2002) 577.
[76] S. Basu, R. Narasimhan, J. Mech. Phys. Sol. 48 (2000) 1967.
[77] S. Basu, R. Narasimhan, Int. J. Solids Struct. 33 (1996) 1191.
[78] K.R. Jayadevan, R. Narasimhan, T.S. Ramamurthy, B. Dattaguru, Int. J. Fract. 116 (2002) 141.
[79] A. Eberle, D. Klingbeil, J. Schicker, Nucl. Eng. Des. 198 (2000) 75.
[80] H. Kurishita, T. Yamamoto, M. Narui, H. Suwarno, T. Kurishita, Y. Yano, M. Yamazaki, H. Matsui, J. Nucl. Mater. 329–333 (2004) 1107.
[81] A. Rossoll, C. Berdin, P. Forget, C. Prioul, B. Marini, Nucl. Eng. Des. 188 (1999) 217.
[82] K.C. Koppenhoefer, R.H. Dodds, Nucl. Eng. Des. 162 (1996) 145.
[83] D.A. Curry, Mater. Sci. Eng. 44 (1980) 285.
[84] D.M. Norris Jr., Eng. Fract. Mech. 11 (1979) 261.
[85] A.J. Rosakis, G. Ravichandran, Int. J. Solids Struct. 37 (2000) 331.
[86] A.I. Ryasanov, S.A. Pavlov, M. Kiritani, Mater. Sci. Eng. A 350 (2003) 245.
[87] M. Komatsu, M. Kiritani, Radiat. Eff. Def. Solids 157 (2002) 75.
[88] Y.B. Xu, Y.L. Bai, Q. Xue, L.T. Shen, Acta Mater. 44 (1996) 1917.
[89] A.T. Zehnder, A.J. Rosakis, J. Mech. Phys. Solids 39 (1991) 385.
[90] M. Kiritani, Y. Satoh, Y. Kizuka, K. Arakawa, Y. Ogasawara, S. Arai, Y. Shimomura, Philos. Mag. Lett. 79 (1999) 797.
[91] M. Kiritani, J. Nucl. Mater. 276 (2000) 41.
[92] K. Yasunaga, M. Iseki, M. Kiritani, Mater. Sci. Eng. A 350 (2003) 76.
[93] M. Kiritani, Mater. Sci. Eng. A 350 (2003) 1.
[94] M. Kiritani, Mater. Sci. Eng. A 350 (2003) 63.
[95] J. Schiotz, T. Leffers, B.N. Singh, Philos. Mag. Lett. 81 (2001) 301.
[96] J. Schiotz, T. Leffers, B.N. Singh, Radiat. Eff. Def. Solids 157 (2002) 193.
[97] Y. Arun Roy, R. Narasimhan, P.R. Arora, Acta Mater. 47 (1999) 1587.
[98] A. Pirondi, C. Dalle Donne, Eng. Fract. Mech. 68 (2001) 1385.
[99] S.V. Kamat, J.P. Hirth, Acta Mater. 44 (1996) 201.
[100] H.X. Li, R.H. Jones, J.P. Hirth, D.S. Gelles, J. Nucl. Mater. 233–237 (1996) 258.
[101] A.K. Ghosal, R. Narasimhan, Mech. Mater. 25 (1997) 113.
[102] D. Bhattacharjee, J.F. Knott, Acta Metall. Mater. 42 (1994) 1747.
[103] S.M. Ohr, Mater. Sci. Eng. 72 (1985) 1.
[104] G.E. Lucas, J. Nucl. Mater. 117 (1983) 327.
[105] H. Kurishita, H. Kayano, M. Narui, M. Yamazaki, J. Nucl. Mater. 150 (1987) 194.
[106] R. Kasada, H. Ono, A. Kimura, Fus. Eng. Des. 81 (2006) 981.

[107] T. Misawa, H. Nagata, N. Aoki, J. Ishizaka, Y. Hamaguchi, J. Nucl. Mater. 169 (1989) 225.
[108] S.J. Zinkle, M. Victoria, K. Abe, J. Nucl. Mater. 307–311 (2002) 31.
[109] G.E. Lucas, G.R. Odette, M. Sokolov, P. Spatig, T. Yamamoto, P. Jung, J. Nucl. Mater. 307–311 (2002) 1600.
[110] T. Ishii, M. Ohmi, J. Saito, T. Hoshiya, N. Ooka, S. Jitsukawa, M. Eto, J. Nucl. Mater. 283–287 (2000) 1023.
[111] P. Jung, A. Hishinuma, G.E. Lucas, H. Ullmaier, J. Nucl. Mater. 232 (1996) 186.
[112] G.R. Odette, M. He, D. Gragg, D. Klingensmith, G.E. Lucas, J. Nucl. Mater. 307–311 (2002) 1643.
[113] K. Ehrlich, E.E. Bloom, T. Kondo, J. Nucl. Mater. 283–287 (2000) 79.
[114] A. Moeslang, V. Heinzel, H. Matsui, M. Sugimoto, Fus. Eng. Des. 81 (2006) 863.
[115] E. Daum, K. Ehrlich, S. Jitsukawa, H. Matsui, A. Moeslang, Fus. Eng. Des. 49&50 (2000) 435.
[116] K. Ehrlich, A. Moeslang, Nucl. Instrum. and Meth. B 139 (1998) 72.
[117] E. Daum, P.P. Wilson, U. Fisher, K. Ehrlich, J. Nucl. Mater. 258–263 (1998) 413.
[118] M. Suzuki, M. Eto, Y. Nishiyama, K. Fukaya, M. Saito, T. Misawa, J. Nucl. Mater. 191–194 (1992) 1023.
[119] T. Misawa, T. Adachi, M. Saito, Y. Hamaguchi, J. Nucl. Mater. 150 (1987) 194.
[120] S.H. Chi, J.H. Hong, I.S. Kim, Scripta Metall. Mater. 30 (1994) 1251.
[121] Y. Dai, X.J. Jia, K. Farrell, J. Nucl. Mater. 318 (2003) 192.
[122] J. Foulds, R. Viswanathan, J. Mater. Eng. Perform. 10 (2001) 614.
[123] E. Wakai, H. Ohtsuka, S. Matsukawa, K. Furuya, H. Tanigawa, K. Oka, S. Ohnuki, T. Yamamoto, F. Takada, S. Jitsukawa, Fus. Eng. Des. 81 (2006) 1077.
[124] E. Wakai, S. Jitsukawa, H. Tomita, K. Furuya, M. Sato, K. Oka, T. Tanaka, F. Takada, T. Yamamoto, Y. Kato, Y. Tayama, K. Fhiba, S. Ohnuki, J. Nucl. Mater. 343 (2005) 285.
[125] Y. Dai, P. Marmy, J. Nucl. Mater. 343 (2005) 247.
[126] X.J. Jia, Y. Dai, J. Nucl. Mater. 323 (2003) 360.
[127] T. Misawa, H. Sugawara, R. Miura, Y. Hamaguchi, J. Nucl. Mater. 133&134 (1985) 313.
[128] M.C. Kim, Y.J. Oh, B.S. Lee, Nucl. Eng. Des. 235 (2005) 1799.
[129] Y. Ruan, P. Spätig, M. Victoria, J. Nucl. Mater. 307–311 (2002) 236.